J. Fluid Mech. (1990), *vol.* 210, *pp.* 201–221
Printed in Great Britain

The concentration distribution produced by shear dispersion of solute in Poiseuille flow

By A. N. STOKES[1] AND N. G. BARTON[2]

[1]CSIRO Division of Mathematics and Statistics, Private Bag Number 10, Clayton, Vic., Australia 3168

[2]CSIRO Division of Mathematics and Statistics, PO Box 218, Lindfield, NSW, Australia 2070

(Received 26 October 1987 and in revised form 15 June 1989)

One of G. I. Taylor's most famous papers concerns the large-time behaviour of a cloud of soluble matter which has been injected into a solvent in laminar flow in a pipe. In the past thirty years, a number of successful attempts have been made to derive differently or extend Taylor's result, which is that the cloud of solute eventually takes a Gaussian profile in the flow direction. The present paper is another examination of this well-worked problem, but this time from the viewpoint of a formal integral transform representation of the solution. This approach leads to a better understanding of the solution; it also enables efficient numerical computations, and leads to extended and new asymptotic expansions.

A Laplace transform in time and a Fourier transform in the flow direction leaves a complicated eigenvalue problem to be solved to give the cross-sectional behaviour. This eigenvalue problem is examined in detail, and the transforms are then inverted to give the concentration distribution. Both numerical and asymptotic methods are used. The numerical procedures lead to an accurate description of the concentration distribution, and the method could be generalized to compute dispersion in general parallel flows. The asymptotic procedures use two different classes of eigenvalues to give leading- and trailing-edge approximations for the solute cloud at small times. Meanwhile, at larger times, one eigenvalue branch dominates the solution and Taylor's result is recovered and extended using the computer to generate extra terms in the approximation. Sixteen terms in the approximation are calculated, and a continued fraction expansion is deduced to enhance the accuracy.

1. Introduction

G. I. Taylor's most cited paper was published in 1953 and is concerned with the shear dispersion of a passive solute injected into a solvent in laminar flow in a straight horizontal pipe. Taylor's celebrated result was that any finite cloud of solute eventually becomes uniformly spread out over the cross-section of the flow and takes up a Gaussian profile in the flow direction. Shear dispersion theory has application to a number of fields including environmental fluid mechanics, chemistry, biology, engineering; and the beautifully simple large-time approximation that Taylor produced has been developed and embellished by many investigators in the last thirty years. The most notable developments of Taylor's asymptotic theory are due to Aris (1956), Philip (1963*a*, *b*), Chatwin (1970), Gill & Sankarasubramanian (1970), de Gance & Johns (1978*a*, *b*) and Smith (1981, 1987). The derivation of asymptotic approximations has been accompanied by experimental work on shear dispersion

(e.g. Plumb *et al.* 1983) and numerical computations (e.g. Gill & Ananthakrishnan 1967; Houseworth 1984; Stokes & Barton 1985; Barton & Stokes 1986).

The object of the present paper is to re-examine Taylor's well-worked problem from a fresh viewpoint. It is observed that the shear dispersion problem is linear, provided that the solute has neutral buoyancy and the diffusivity of the solute is independent of concentration, and therefore the governing equation can be attacked using integral transforms. Specifically, the governing parabolic partial differential equation is Laplace transformed in time and Fourier transformed in the flow direction, and this gives an eigenvalue problem for the cross-sectional dependence of the transform of the concentration distribution. The eigenvalue problem is examined both numerically and asymptotically, and calculations are made of the concentration distribution.

The treatment of the problem by integral transforms has several attractive features: it enables a unified theory to be presented for the dispersion of passive solute in Poiseuille flow, it can form the basis for new asymptotic approximations and extremely efficient numerical schemes, it is capable of modification for other flows (such as the plane Poiseuille flow with cross-sectional drift described by Jayaraj & Subramanian 1978), and it clears up confusion over anomalous results reported by Barton (1983).

Section 2 of the paper contains mathematical preliminaries dealing with the definition of the integral transforms, the derivation of the crucial eigenvalue problem, and the formal inversion of the transforms using residue calculus. The eigenvalue problem is solved numerically in §3, and the transforms are inverted by a combined analytical and numerical procedure to give the concentration distribution. Sections 4, 5 and 6 follow the same transform procedure using approximations to the eigenfunctions. A local approximation near the origin in the transformed space is used in §5 to obtain large-time approximations, whilst in §6, the rather complicated large parameter asymptotic behaviour is analysed to yield regional approximations for small time. Of these, the trailing-edge approximation appears to be new. The regions of validity of the various approximations overlap to an extent sufficient to provide a complete picture of the solution.

We conclude this introduction by emphasizing the main features of the paper. It is possible to use integral transforms to analyse shear dispersion in parallel flows in general and in Poiseuille flow in particular. The resulting numerical method is straightforward to implement, and can be made to give better accuracy than the alternatives. The analysis of eigenfunctions gives an interesting association between types of asymptotic behaviour in the transform variables and behaviour of the concentration distribution in various regions. Finally, use of the eigenvalues in approximations provides an analytic alternative to the more time-consuming numerical methods, as well as some insight into the qualitative behaviour of the solutions.

2. Mathematical preliminaries: integral transforms and the eigenvalue problem

We consider the parabolic partial differential equation

$$\frac{\partial C}{\partial t}+(1-2r^2)\frac{\partial C}{\partial x}=\frac{1}{r}\frac{\partial}{\partial r}\left(r\frac{\partial C}{\partial r}\right)+P^{-2}\frac{\partial^2 C}{\partial x^2} \tag{1}$$

subject to the conditions

$$\partial C/\partial r = 0 \quad \text{at} \quad r = 0, 1,$$

$$x^n C \to 0 \quad \text{as} \quad x \to \infty, \quad n = 0, 1, \ldots,$$

$$C(r, x, 0; P) = C_0(r, x).$$

This problem describes, in dimensionless coordinates moving at the discharge speed of the flow, the axially symmetric dispersion of a cloud of passive solute which has been injected into a solvent in laminar flow in a straight horizontal pipe. Problem (1) is attacked in the present paper using a Fourier transform in the axial coordinate x and a Laplace transform in time t. Accordingly, define the Fourier transform of $C(r, x, t; P)$ by

$$\Phi(r, \lambda, t; P) = \int_{-\infty}^{\infty} e^{-i\lambda x} C(r, x, t; P)\, dx$$

and take the Fourier transform of (1) to obtain

$$\frac{\partial \Phi}{\partial t} + i\lambda(1-2r^2)\,\Phi = \frac{1}{r}\frac{\partial}{\partial r}\left(r\frac{\partial \Phi}{\partial r}\right) - \lambda^2 P^{-2}\Phi,$$

$$\frac{\partial \Phi}{\partial r} = 0 \quad \text{at} \quad r = 0, 1, \qquad \Phi(r, \lambda, 0; P) = \int_{-\infty}^{\infty} e^{-i\lambda x} C_0(r, x)\, dx.$$

The Péclet-number dependence can now be removed by writing

$$\Phi(r, \lambda, t; P) = f(r, \lambda, t)\, e^{-t\lambda^2 P^{-2}} \tag{2}$$

in which $f(r, \lambda, t)$ is the (infinite-Péclet-number) solution of

$$\frac{\partial f}{\partial t} + i\lambda(1-2r^2) f = \frac{1}{r}\frac{\partial}{\partial r}\left(r\frac{\partial f}{\partial r}\right),$$

$$\frac{\partial f}{\partial r} = 0 \quad \text{at} \quad r = 0, 1, \qquad f(r, \lambda, 0) = \int_{-\infty}^{\infty} e^{-i\lambda x} C_0(r, x)\, dx.$$

We now define the Laplace transform of $f(r, \lambda, t)$ by

$$F(r, \lambda, \omega) = \int_0^{\infty} e^{-\omega t} f(r, \lambda, t)\, dt,$$

where $F(r, \lambda, \omega)$ is the solution of the problem

$$\frac{d^2F}{dr^2} + \frac{1}{r}\frac{dF}{dr} - [\omega + i\lambda(1-2r^2)]\,F = -f(r, \lambda, 0), \tag{3}$$

$$dF/dr = 0 \quad \text{at} \quad r = 0, 1.$$

Let $A(r, \lambda, \omega)$ and $B(r, \lambda, \omega)$ be two solutions of the homogeneous form of (3) subject to the boundary conditions

$$A = 1 \text{ and } dA/dr = 0 \quad \text{at} \quad r = 0 \quad \text{for all } (\lambda, \omega),$$

$$B = 1 \text{ and } dB/dr = 0 \quad \text{at} \quad r = 1 \quad \text{for all } (\lambda, \omega).$$

The solution of (3) is given by

$$F(r, \lambda, \omega) = B(r, \lambda, \omega) \int_0^r \frac{A(s, \lambda, \omega) f(s, \lambda, 0)}{W(s, \lambda, \omega)}\, ds + A(r, \lambda, \omega) \int_r^1 \frac{B(s, \lambda, \omega) f(s, \lambda, 0)}{W(s, \lambda, \omega)}\, ds,$$

where the Wronskian $W(r,\lambda,\omega)$ is found to be

$$W(r,\lambda,\omega) = A'(1,\lambda,\omega)/r,$$

in which a prime denotes differentiation with respect to r.

Now $A(r,\lambda,\omega)$, $B(r,\lambda,\omega)$ and $f(r,\lambda,0)$ are entire functions of λ and ω, and so the transformed concentration $F(r,\lambda,\omega)$ is analytic everywhere except for poles at zeros of the Wronskian, that is, where

$$A'(1,\lambda,\omega) = 0. \tag{4}$$

Therefore, the homogeneous form of (3) defines an eigenvalue problem in which the eigenvalue ω depends on the parameter λ so as to satisfy (4). Define the eigenvalue branches by $\omega_n(\lambda)$, $n = 1,\ldots$.

The Fourier and Laplace transforms are now inverted using residue calculus to give the concentration distribution $C(r,x,t;\infty)$ for infinite Péclet numbers. (The case for finite Péclet numbers is explained below.) Formally, we have

$$C(r,x,t;\infty) = -\frac{\mathrm{i}}{4\pi^2}\int_{-\infty}^{\infty} \mathrm{e}^{\mathrm{i}\lambda x}\int_{\Gamma} \mathrm{e}^{\omega t} F(r,\lambda,\omega)\,\mathrm{d}\omega\,\mathrm{d}\lambda$$

in which the contour Γ may depend on λ but should enclose the poles of $F(r,\lambda,\omega)$ for each λ. Then the integration with respect to ω may be achieved by summing the residues at the poles to give

$$C(r,x,t;\infty) = \frac{1}{2\pi}\int_{-\infty}^{\infty} \mathrm{e}^{\mathrm{i}\lambda x}\,\Psi(r,\lambda,t)\,\mathrm{d}\lambda, \tag{5}$$

in which $\Psi(r,\lambda,t)$ is the series

$$\Psi(r,\lambda,t) = \sum_{n=1}^{\infty} \mathrm{e}^{\omega_n(\lambda)t} F_n(r,\lambda,\omega_n(\lambda)) \tag{6}$$

with each term F_n given by the residue of $F(r,\lambda,\omega)$ at ω_n; that is,

$$F_n(r,\lambda,\omega_n(\lambda)) = -\lim_{\omega\to\omega_n} F^2(\partial F/\partial\omega)^{-1}. \tag{7}$$

Equations (5)–(7) give a way of computing the concentration $C(r,x,t;\infty)$ provided that the series (6) converges and the resulting sum is integrable.

Equation (2) is a device for removing the Péclet number; the modified problem is one of infinite Péclet number, where axial diffusion is negligible. As Taylor (1953) remarked, this approximation is often justified, but where it is not, the solution for finite number can be recovered by convolution:

$$C(r,x,t;P) = (\pi t)^{-\frac{1}{2}}\tfrac{1}{2}P\int_{-\infty}^{\infty} C(r,x-X,t;\infty)\,\mathrm{e}^{-X^2P^2/4t}\,\mathrm{d}X. \tag{8}$$

The effect of axial diffusion in (1) is accounted for by finite Péclet number. Thus the profiles become smoother with decreasing Péclet number.

3. Computation of the concentration distribution

The evaluation of the concentration distribution $C(r,x,t;\infty)$ for infinite Péclet number proceeds in three stages. First, the roots $\omega_n(\lambda)$ of (4) have to be found by an iterative process; then the residues $F_n(r,\lambda,\omega_n(\lambda))$ have to be evaluated; and, finally, the Fourier inversion (5) has to be performed numerically.

The roots $\omega_n(\lambda)$ of $A'(1,\lambda,\omega)=0$ are found by the Newton–Raphson procedure

$$\omega_n^{k+1}=\omega_n^k-A'(1,\lambda,\omega_n^k)/A'_\omega(1,\lambda,\omega_n^k),\quad k=0,1,2,\ldots. \tag{9}$$

The values of $A'_\omega(1,\lambda,\omega)$ which were required in this procedure were obtained by numerically solving the inhomogeneous equation

$$\frac{\mathrm{d}^2A_\omega}{\mathrm{d}r^2}+\frac{1}{r}\frac{\mathrm{d}A_\omega}{\mathrm{d}r}-[\omega+\mathrm{i}\lambda(1-2r^2)]A_\omega=A$$

(obtained by differentiating the homogeneous form of (3) partially with respect to ω) under the homogeneous initial conditions

$$\mathrm{d}A_\omega/\mathrm{d}r=A_\omega=0\quad\text{at}\quad r=0.$$

The initial-value problems determining $A(r,\lambda,\omega)$ and $A_\omega(r,\lambda,\omega)$ were solved by a Taylor series procedure using a 50-point grid. The procedure (9) usually only required one or two iterations since λ was regularly incremented and excellent starting estimates were available. Starting estimates for $\lambda=0$ were obtained analytically. For $\lambda=0$, $A(r,\lambda,\omega)$ satisfies the equation

$$r^2\frac{\mathrm{d}^2F}{\mathrm{d}r^2}+r\frac{\mathrm{d}F}{\mathrm{d}r}-r^2\omega F=0$$

under the homogeneous boundary conditions $A'(0,0,\omega)=A'(1,0,\omega)=0$ (the former by construction and the latter in order to give the eigenvalues). The solutions for $\lambda=0$ are $A(1,\lambda,\omega)=J_0(j'_nr)$, and the eigenvalues for $\lambda=0$ are $\omega_n=-j'^2_n$, $n=1,2,\ldots$ where the j'_n are the zeros of J'_0 (noting that $j'_0=0$). This argument provides a sequence of starting points for the various branches and serves to enumerate them: thus branch 1 originates from $(\lambda=0,\omega=0)$ and branch n $(n\geqslant 2)$ originates from $(\lambda=0,\omega=-j'^2_{n-1})$.

Figure 1 shows trajectories of the first six zeros of $A'(1,\lambda,\omega)$ for real positive λ. Each crosses the real axis at $\lambda=0$ as explained above and follows a path for λ negative which is the mirror image in the negative real ω-axis. Figure 1 does not show the λ-values, so one cannot be sure that the real part of $\omega_n(\lambda)$ diminishes with n for each fixed λ. However, it is clear that the real part of each $\omega_n(\lambda)$ has an upper bound (for each n and any λ) which is negative, and this ensures the convergence of (6) since the residues F_n are not exponentially large. In practice, the rate of convergence of (6) increases with t and it was usually sufficient to restrict attention to the first six branches.

The next step is concerned with the evaluation of the residues $F_n(r,\lambda,\omega_n(\lambda))$ defined by (7). In fact, the use of the property

$$\lim_{\omega\to\omega_n}A(r,\lambda,\omega)=B(r,\lambda,\omega_n)A(1,\lambda,\omega_n)$$

and simple manipulations of the integral representation of $F(r,\lambda,\omega)$ give that

$$F_n(r,\lambda,\omega_n)=\frac{A(r,\lambda,\omega_n)\displaystyle\int_0^1 A(s,\lambda,\omega_n)f(s,\lambda,0)\,s\,\mathrm{d}s}{A'_\omega(1,\lambda,\omega_n)A(1,\lambda,\omega_n)}.$$

The final stage of the computation is the numerical evaluation of the Fourier inversion integral (5). A difficulty here is that the integrand along the real λ-axis is oscillatory. This difficulty remains if the summation in (6) is performed before

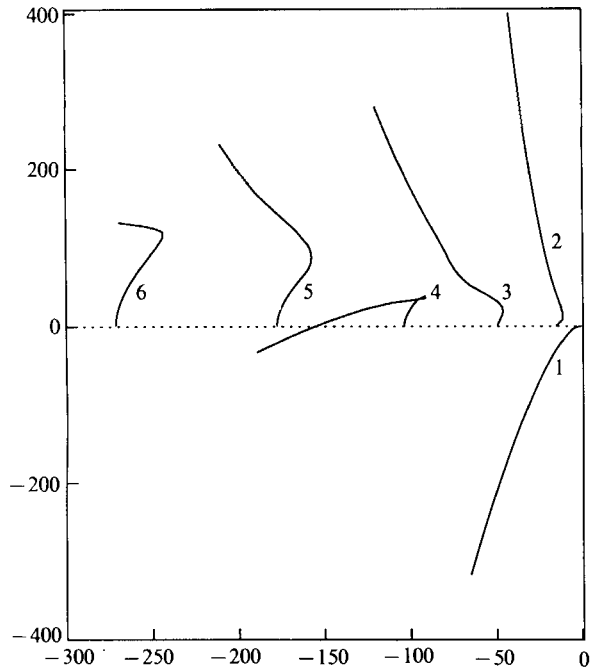

FIGURE 1. Trajectories of the eigenvalues ω for λ real and positive.

attempting the inversion integral, and the oscillations are then disordered. The oscillations are caused by fairly rapid change in the exponents $i\lambda x+\omega_n(\lambda)t$ of the terms in (5), (6). Fortunately, the contributions from individual terms can be integrated over quite long intervals by linearly interpolating the exponent. Thus, to integrate $\exp(f(\lambda))$ from λ_1 to λ_2, we use the approximation

$$\int_{\lambda_1}^{\lambda_2} \exp\left[f(\lambda_1)+\frac{f(\lambda_2-f(\lambda_1)}{\lambda_2-\lambda_1}(\lambda-\lambda_1)\right]\mathrm{d}\lambda = \frac{\mathrm{e}^{f(\lambda_2)}-\mathrm{e}^{f(\lambda_1)}}{f(\lambda_2)-f(\lambda_1)}(\lambda_2-\lambda_1).$$

Similarly simple approximations were employed near a stationary point of $f(\lambda)$. The inversion procedure is also simplified by the fact that the contributions from higher eigenvalues $\omega_n(\lambda)$ are small and only significant over a small range of λ.

Computations were carried out for the case in which the initial distribution of solute is a pulse uniformly spread over the cross-section of the pipe; that is,

$$C_0(r,x) = \delta(x) \tag{10}$$

which implies that $f(r,\lambda,0) = 1.$

For convenience of presentation, results are given for the cross-sectional integral

$$\bar{C}(x,t;P) = 2\int_0^1 rC(r,x,t;P)\,\mathrm{d}r \tag{11}$$

in which the integration over the cross-section was performed before attempting the Fourier inversion (5)–(7); that is,

$$\bar{C}(x,t;\infty) = \frac{1}{2\pi}\sum_{n=1}^{\infty}\int_{-\infty}^{\infty}\bar{F}_n(\lambda,\omega_n(\lambda))\,\mathrm{e}^{\mathrm{i}\lambda x+\omega_n(\lambda)t}\,\mathrm{d}\lambda, \tag{12}$$

in which $\bar{F}_n$ is

$$\bar{F}_n(\lambda, \omega_n(\lambda)) = \frac{\left(\int_0^1 A(s, \lambda, \omega_n)\, s\, \mathrm{d}s\right)^2}{A'_\omega(1, \lambda, \omega_n) A(1, \lambda, \omega_n)}. \tag{13}$$

Figure 2(*a*) shows the profiles $\bar{C}(x, t; \infty)$ for infinite Péclet numbers and at various dimensionless times. At the applicable times, the results agree approximately with those of Gill & Ananthakrishnan (1967) derived using finite-difference methods from a slightly different initial condition, and with those of Houseworth (1984) derived using a Monte-Carlo method. The results also agree with those of Barton & Stokes (1966) derived using a hybrid numerical method. Figure 2(*b*) shows the concentration distribution for various Péclet numbers at the dimensionless time $t = 0.05$. These computations were made using the convolution integral (8). The distribution of solute at large time clearly approaches the Gaussian curve proposed by Taylor (1953). For infinite Péclet number, however, the distribution is band-limited, and the inconsistency of this requirement with the Gaussian form is evident at small times.

4. Approximations and the complex plane

Approximations are developed for both small and large time in the following sections. The pattern is similar in each case. An appropriate approximation is developed for $A(r, \lambda, \omega)$ and used in the eigenvalue condition (4) to give one of the variables as a function of the other. After various manipulations, the representation (5), (6) takes the form of a series multiplied by the exponential of the two most significant terms of the series derived from the original exponent $(\omega t + \mathrm{i}\lambda x)$. The integral (5) can then be evaluated directly.

Three regions are approximated in this way. They are the central region for large time, and the leading and trailing edges for small time. As will be shown, the regions of validity of these approximations merge to give a reasonably complete description of all the features of interest in the solution.

To derive accurate approximations of this kind, it is useful to deform the integration contour into a steepest-descent contour passing through a saddle point of the integrand. If the proposed approximation to the integrand is good along the part of such a contour where it is large enough to affect the overall integral, then the resulting integral will be accurate.

As described above, $\omega(\lambda)$ has a number of branches, and these meet at branch points in the complex plane. These are also branch points of the integrand, and they are its only singularities in the finite plane. These branch points are plotted in figure 3. Their significance is that they mark the boundaries of regions of relatively smooth behaviour in which the various approximations may be applied.

A knowledge of the location of the branch points is also useful if the numerical integration on the real λ-axis proves to be difficult. This happens near the ends of the profile, and the best solution is to move to a more appropriate contour, of which the ideal is a steepest-descent path of the type mentioned above. In the calculations presented above, sufficient accuracy was obtained by integrating on the real axis alone, although calculations on other contours were done as a check.

There is a connection between the rather sudden changes in the curves of figure 1 and the branch points plotted in figure 3. The trajectories in figure 1 are the images of the imaginary axis in figure 3 (i.e. the *real* λ-axis), and there are several branch points lying quite close to that axis. There is one at (12.395, 126.93), which is very

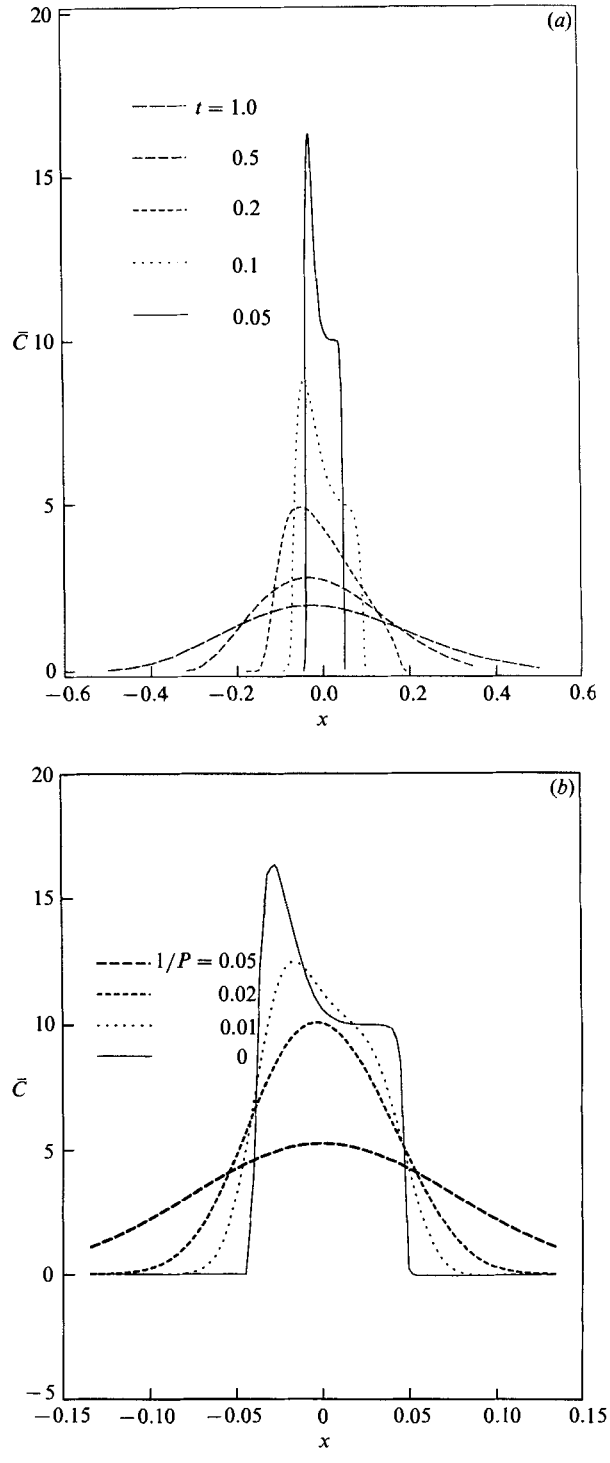

FIGURE 2. Profiles $\bar{C}$ for (*a*) Péclet number $P = \infty$ and various values of t; (*b*) $t = 0.05$ and various values of P.

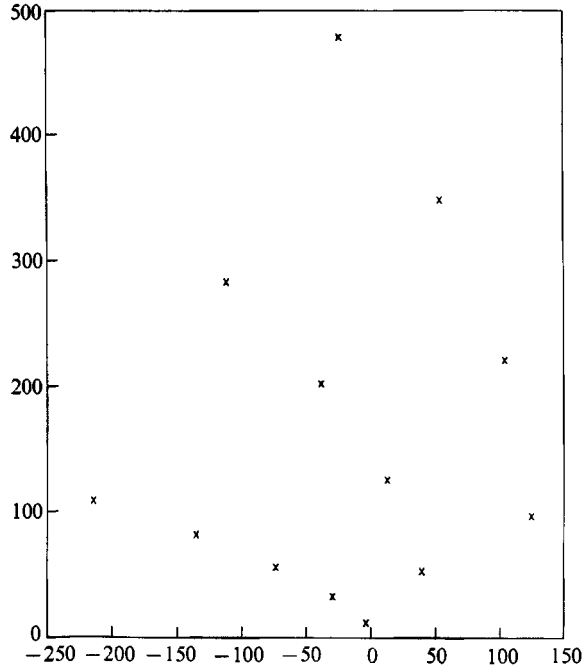

FIGURE 3. Branch points of ω when expressed as a function of λ. Note that there are infinitely many branches, and only two meet at each point.

close indeed, and is responsible for the very sharp turn of curve 4 in figure 1. In this neighbourhood there is a change from one type of behaviour (type II of §6) to one of two types that will be followed thereafter (type I or III). Which type emerges depends on which side of the branch point the trajectory passes.

This changeover was noted by Barton (1983), who also focused on a region near (12.395, 126.93), although his parametrization was slightly different. Since only one type of behaviour (I) was then expected, the appearance of type III behaviour was considered 'anomalous'.

5. Approximations for large time

We begin by using our Fourier–Laplace transform approach to extend Taylor's (1953) approximation. The derivation can be done mechanically by computer, and many extra coefficients calculated. For large time, the first term in the representation (5), (6) is exponentially large in comparison with the other terms. Thus, an approximation to the solution is

$$\bar{C}(x,t;\infty) = \frac{1}{2\pi}\int_{-\infty}^{\infty} \bar{F}_1(\lambda,\omega_1(\lambda))\,\mathrm{e}^{\mathrm{i}\lambda x+\omega_1(\lambda)t}\,\mathrm{d}\lambda, \tag{14}$$

in which $\omega_1(\lambda)$ is the eigenvalue branch which emanates from $\lambda = 0$, $\omega = 0$. The integral (14) is now approximated using Laplace's stationary-point method.

If the solution $A(r,\lambda,\omega)$ of the homogeneous form of (3) is expressed as a power series in r, the coefficients are polynomials in λ (or more conveniently, $\Lambda = \mathrm{i}\lambda$) and ω. The first few terms are

$$A(r,\Lambda,\omega) = 1+(\Lambda+\omega)\,r^2/4+r^4[(\omega+\Lambda)^2-8\Lambda]/64+\ldots. \tag{15}$$

n/m	0	1	2	3	4	5
0	1	0	0	0	0	0
1	0	0.83333	0	0	0	0
2	−0.138888	−0.381324	0.347222	0	0	0
3	−0.0527033	−0.397858	−0.317770	0.0964506	0	0
4	0.0330472	0.0208640	−0.210619	−0.132404	0.0200938	0
5	0.0344749	0.175368	0.143264	−0.0507667	−0.0367789	0.003349

TABLE 1. Table of coefficients $10^{m+n}a_{nm}$ for Taylor–Chatwin large-time approximation.

The quantity $A')r, \Lambda, \omega)$ can be represented as the series

$$A'(1,\lambda,\omega) = \omega/4 - \Lambda^2/192 + \omega^2/32 - \Lambda\omega/96 - \Lambda^3/7680 - 4300(\Lambda/256)^4 - 11/180\omega(\Lambda/16)^2\ldots, \quad (16)$$

and setting this to zero (as in the eigenvalue condition (4)) and solving for ω gives

$$\omega_1(\Lambda) = \Lambda^2/48 - \Lambda^3/2880 - 41\Lambda^4/(63\times 40960) + 13\Lambda^5/11059200\ldots.$$

These results can be substituted in (13) to give $\bar{F}_1(\lambda,\omega(\lambda))$,

$$\bar{F}_1(\lambda,\omega(\lambda)) = 1 - \Lambda^2/720 + 17\Lambda^3/322560 + 307\Lambda^4/92897280\ldots.$$

Finally, (14)–(16) give the mean concentration

$$\bar{C}(x,t;\infty) = \frac{1}{2\pi i}\int_{-i\infty}^{i\infty}(1 - \Lambda^2/720 + 17\Lambda^3/322560 + t\Lambda^3/2880\ldots)\,e^{\Lambda x + \Lambda^2 t/48}\,d\Lambda, \quad (17)$$

in which the first two terms in the exponent have been retained and the rest expanded as a series in t and Λ. It now remains to integrate (17) term by term. We use the substitutions $T = (t/24)^{\frac{1}{2}}$, $X = x/T$ and $u = \Lambda T$ to obtain

$$\bar{C}(x,t;\infty) = \frac{2}{\pi i T}\int_{-i\infty}^{i\infty}\left[1 - \frac{u^3T^{-1}}{120} + \left[\frac{u^6}{40} - \frac{123u^4}{448} - u^2\right]\frac{T^{-2}}{720} - \left[\frac{u^9}{225} - \frac{41u^7}{140} - \frac{11u^5}{6} - \frac{17u^3}{7}\right]\frac{T^{-3}}{46080} + \ldots\right]e^{u^2/2 + Xu}\,du$$

in which the various terms can be evaluated using the standard results

$$\frac{1}{2\pi i}\int_{-i\infty}^{i\infty} u^n e^{u^2/2 + Xu}\,du = (2\pi)^{-\frac{1}{2}}\frac{d^n}{dX^n}e^{-X^2/2} = (2\pi)^{-\frac{1}{2}}(-1)^n e^{-X^2/2}\,\mathrm{He}_n(X),$$

where He, implicitly defined by this expression, is a Hermite polynomial.

The fact that the algebra in the above approach is systematically reduced to series operations means that the labour can be delegated to a computer, and we have extended the series to order T^{-16} to obtain

$$\bar{C} \sim (2\pi)^{-\frac{1}{2}}e^{-X^2/2}\sum_{n=0}^{5}\frac{1}{T^{n+1}}\sum_{m=0}^{n}a_{nm}\,\mathrm{He}_{2m+n}(X). \quad (18)$$

Some of the coefficients are recorded in table 1, and the terms up to order T^{-3} agree with Chatwin's (1970) improved version of Taylor's result.

A comparison of the profiles calculated using this series, for $t = 0.2$, 0.5 and 1.0 is

shown in figure 4. The approximation behaves as an asymptotic series in that the terms eventually become large, and it is important to stop summing at some appropriate time. We avoided this difficulty by converting the series to a continued fraction expansion in $1/T$. These expansions do not have the tendency of the series to diverge after a certain point, and so gave a fairly modest improvement in accuracy, and much added convenience.

The approximation is excellent for $t \geqslant 0.5$, but is not very good for $t = 0.2$ and X negative, although curiously it is quite good for X positive. The accuracy is limited essentially by the rate of convergence of the series (16) for ω, and this is governed by the proximity of the branch point $(-3.866, 13.199)$ (see figure 3).

An alternative approach, used by Philip (1963*a*, *b*), can adequately approximate the solution including the branch points. He dealt with what was in effect a rational function equivalent to the series for ω in terms of λ, and equated truncated parts of the numerator to zero. The various roots corresponded to our branches, and the early parts of the trajectories in his figure 3 correspond to ours in figure 1. An equivalent approach here is to truncate (15) and solve for the various zeros of the polynomial in ω, given λ. This does not lead to an expression which can be explicitly integrated, but can be substituted in (14), followed by numerical integration. If the contour for this last stage is well chosen, the result is an improvement on the use of (18). However, the choice of contour depends on the values of x and t, so the implementation is more complicated.

6. Approximations for small time

At small times, different types of approximation are required near the leading and trailing edge. When x and t are small, the dominant contribution to (5), (6) is derived using an asymptotic expansion for λ, ω large. In particular, it is necessary to find asymptotic expansions for the eigenvalues $\omega(\lambda)$ for large λ. Note that the eigenvalues displayed in figure 1 behave curiously in that all except the first move initially into the upper half-ω-plane, but the fourth and sixth subsequently reverse direction and move into the lower half-plane. It will be shown that the behaviour of one class of eigenfunctions (branches 1, 4 and 6 on figure 1) determines the leading edge of the solute cloud at small times, whilst another class (branches 2, 3 and 5) is associated with the trailing edge.

Consider the homogeneous form of (3) under homogeneous boundary conditions

$$\mathrm{d}F/\mathrm{d}r = 0 \quad \text{at} \quad r = 0, 1.$$

We make the substitution $s = r^2$ to find the following equation for $F(s, \lambda, \omega)$:

$$4\left[s\frac{\mathrm{d}^2F}{\mathrm{d}s^2} + \frac{\mathrm{d}F}{\mathrm{d}s}\right] = (\omega + \mathrm{i}\lambda - 2\mathrm{i}\lambda s)F$$

The solution for F is

$$F(s) = \mathrm{e}^{-bs/2}M(a, 1, bs) \tag{19}$$

where M is the confluent hypergeometric function, and

$$b = (-2\mathrm{i}\lambda)^{\frac{1}{2}}, \quad a = \tfrac{1}{2} + \frac{\omega + \mathrm{i}\lambda}{4b}.$$

The small-time approximation requires an asymptotic expansion of $F(s(\lambda))$ for λ

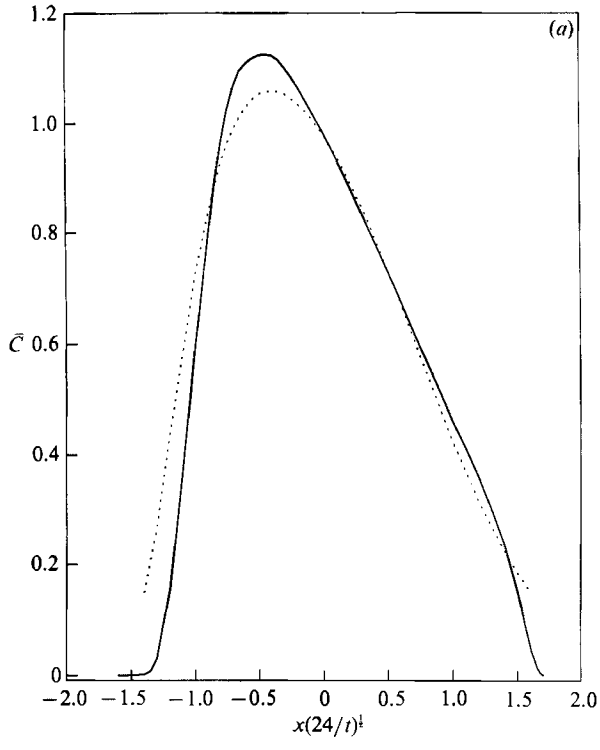

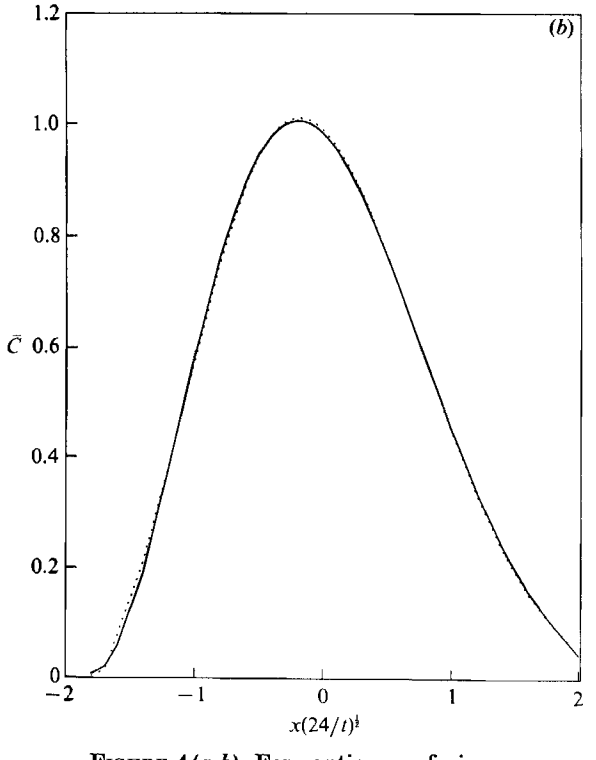

FIGURE 4(*a*,*b*). For caption see facing page.

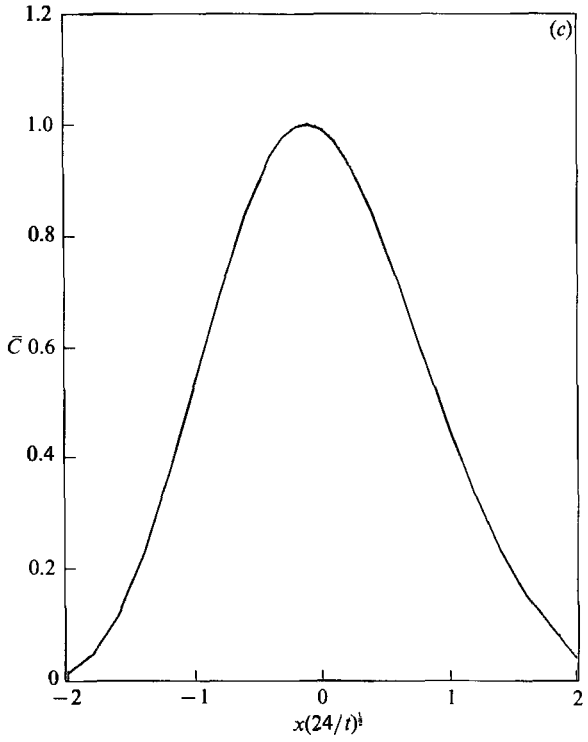

FIGURE 4. The Taylor–Chatwin approximation for large time, plotted at (*a*) $t = 0.2$, (*b*) 0.5 and (*c*) 1.0 compared with the profiles calculated by numerical integration. The horizontal axis is the normalized variable $x(24/t)^{\frac{1}{2}}$, corresponding to 'standard deviations' of the eventual Gaussian form. ....., Taylor approximation; ——, true profile.

large. By standard results for the confluent hypergeometric function (Abramowitz & Stegun 1965, 13.5.19), we have that, as $\lambda \to \infty$,

$$M(a, 1, bs) \sim e^{bs/2}(1-2a)^{-\frac{1}{3}}[\mathrm{Ai}(\tau')\cos(a\pi) + \mathrm{Bi}(\tau')\sin(a\pi)],$$

where

$$\tau' = \left(\frac{bv}{2-4a} - 1\right)(1-2a)^{\frac{2}{3}}$$

and Ai and Bi are the Airy functions. We use a slightly more accurate version with

$$\tau' = (\tfrac{3}{2}(\tfrac{1}{2}-a)(\sinh 2\theta - 2\theta))^{\frac{2}{3}}, \quad \text{where} \quad \cosh^2\theta = bs/(2-4a). \tag{20}$$

In this form it is consistent with the WKB approximation (Abramowitz & Stegun 1965, 13.5.16) when τ' is large.

The derivative $\mathrm{d}F/\mathrm{d}r$ is then

$$\mathrm{d}F/\mathrm{d}r \approx -b^2(1-2a)^{-\frac{2}{3}}[\mathrm{Ai}'(\tau')\cos(a\pi) + \mathrm{Bi}'(\tau')\sin(a\pi)]$$

and the eigenvalues are approximately the zeros of this expression when $s = 1$ and τ is the corresponding value of τ'. To see where the eigenvalues are found, it is useful to study the asymptotic behaviour of the Airy functions. We have

$$\mathrm{Ai}'(x) \approx \frac{1}{2\pi^{\frac{1}{2}}} x^{\frac{1}{4}} e^{-2x^{\frac{3}{2}}/3}, \quad \arg(x) < \pi,$$

and this suggests a division of the τ-plane into three equal sectors. Sector I is the region $|\arg(\tau)| < \frac{1}{3}\pi$, sector II the region $\frac{1}{3}\pi < \arg(\tau) < \pi$, and sector III the region

$-\pi < \arg(\tau) < -\frac{1}{3}\pi$. The function $\mathrm{Ai}'(x)$ is rapidly diminishing in the interior of sector I, and increasing in sectors II and III. It is real and oscillatory on the real negative axis which separates II and III, and there all the zeros of Ai and Ai′ are found. There is symmetry based on rotation by $\frac{2}{3}\pi$ radians, and this can be exploited by defining

$$A_1(x) = \mathrm{Ai}(x), \quad A_2(x) = v^2\,\mathrm{Ai}(v^2x), \quad A_3(x) = v\mathrm{Ai}(vx), \quad \text{where} \quad v = \mathrm{e}^{2\pi\mathrm{i}/3}.$$

Then $A_1(x)+A_2(x)+A_3(x) = 0$, for any x, and A_2, A_3 are diminishing solutions in sectors II and III respectively.

Using the relations $\mathrm{Ai}'(x) = -A_2'(x)-A_3'(x)$, $\mathrm{Bi}'(x) = \mathrm{i}(A_2'(x)-A_3'(x))$ the approximate eigenvalue criterion may be written:

$$\mathrm{e}^{-\mathrm{i}a\pi}A_2'(\tau)+\mathrm{e}^{\mathrm{i}a\pi}A_3'(\tau) \approx 0 \quad \text{or} \quad \mathrm{e}^{2a\mathrm{i}\pi} \approx -A_2'(\tau)/A_3'(\tau).$$

In this last criterion, the behaviour of both sides is simplified over large sectors. For example, in sector I of the τ-plane, $A_2'+A_3' \approx 0$, and so $\mathrm{e}^{2a\mathrm{i}\pi} \approx 1$, or a is approximately an integer. This is called the type I condition. In sector II,

$$A_2'(\tau)/A_3'(\tau) \approx \mathrm{i}\mathrm{e}^{4/3\tau^{\frac{3}{2}}}$$

so $\mathrm{i}\pi(a-\frac{1}{4}) \approx \frac{4}{3}\tau^{\frac{3}{2}}$. This is a type II condition. The condition within sector III is essentially the same. Conversely, if a lies well within the upper half-plane, i.e. $\mathrm{Im}(a) \gg 0$, then $A_2'(\tau)/A_3'(\tau) \approx 0$. This is true when τ is within sector II, but it is also true if τ is close to a zero of A_2'. This last is called a type III condition.

The association between asymptotic behaviour in the parameters and particular regions of the flow arises through the location of saddle points in the integrand of (5), (6). If an approximation is good in the neighbourhood of a saddle point, and a steepest descent contour is followed in that neighbourhood, then the approximation will determine the approximate value of the integral. Now the approximate location of the saddle point is where the exponent $(\omega t+\mathrm{i}\lambda x)$ is stationary with x and t large, and that is where

$$\partial\mathrm{i}\lambda/\partial\omega \approx -t/x.$$

By substitution, it can be shown that the derivatives in the respective regions are:

$$\text{I.}\ \frac{\partial\mathrm{i}\lambda}{\partial\omega} \approx -1; \quad \text{II.}\ \frac{\partial\mathrm{i}\lambda}{\partial\omega} \approx 0; \quad \text{III.}\ \frac{\partial\mathrm{i}\lambda}{\partial\omega} \approx 1.$$

Type I approximation, then, determines behaviour near the leading edge $x \approx t$, and type III approximation determines it near the trailing edge. Type II approximation is associated with the physically unrealized region $|x| \gg t$.

The curves in figure 1 may now be interpreted. Each, except the first, begins as a type II approximation, and approaches an approximately parabolic region in which there are branch points. Near these branch points, all three kinds of behaviour are found. From there on, each curve enters a region of either type I (curves 1, 4 and 6) or type III (curves 2, 3 and 5) behaviour.

As noted above, the transition to type III behaviour was the 'anomalous' behaviour noted by Barton (1983). The first observation of type III behaviour seems to be in the work of Philip (1963*b*). Here approximate eigenvalues emerge as roots of a sequence of polynomials of increasing order in the slightly different parameters $\mathrm{i}\Omega = \omega-\mathrm{i}\lambda$ and $\lambda' = \lambda/\mathrm{i}\Omega$. The first two roots found when Ω is large are clearly of type I, but the third, which appears with the cubic approximation, does not at all fit in the same pattern. Chatwin (1973) noted that when $\Omega = 100$, $\lambda' \approx 2.32-0.32\mathrm{i}$ for this root in Philip's approximation, whereas his expected Type I version gave

0.85−0.35i, and thought that this was because of a failure in Philip's method. But in fact the type III approximation, calculated from a numerical solution of the differential equation, is $\lambda' = 2.055-1.69\mathrm{i}$, and in the circumstances Philip's value is as good an approximation to this as can be expected.

6.1. *Leading-edge approximation*

With the Type I eigenvalues, we have $e^{2ia\pi} \approx 1$ so that $a \to -n$ $(n = 0, 1, 2, \ldots)$ and

$$\omega \to -\mathrm{i}\lambda - (4n+2)(-2\mathrm{i}\lambda)^{\frac{1}{2}} \quad \text{as} \quad \lambda \to \infty. \tag{21}$$

These eigenvalues were found by Chatwin (1973). Their corresponding eigenfunctions are

$$\phi_n(r, \lambda, \omega_n(\lambda)) = e^{-br^2/2} L_n(br^2), \tag{22}$$

where L_n are the Laguerre polynomials. These functions are large near $r = 0$ and decay towards the boundary, and hence describe the concentration distribution in the central, fast-moving part of the flow. In figure 1, these eigenvalues are labelled 1, 4 and 6 and they correspond to $n = 0, 1, 2$ respectively. These eigenvalue branches are associated with the leading edge of the solute cloud.

Thus the concentration distribution is given by (5), (6), where the residues $F_n(r, \lambda, \omega_n(\lambda))$ are given by

$$F_n(r, \lambda, \omega_n(\lambda)) = \frac{\phi_n(r, \lambda, \omega_n(\lambda)) \int_0^1 r\phi_n(r, \lambda, \omega_n(\lambda)) f(r, \lambda, 0)\, \mathrm{d}r}{\phi'_{n_\omega}(1, \lambda, \omega_n(\lambda))\, \phi_n(1, \lambda, \omega_n(\lambda))}. \tag{23}$$

For the presentation of results, we only consider solute dispersion from a δ-function source as in (10), so that $f(r, \lambda, 0) = 1$. The approximation for the leading edge of the solute cloud then takes the form

$$\bar{C}(x, t; \infty) = \sum_{n=0}^{\infty} \left(\frac{8}{\pi}\right)^{\frac{1}{2}} (t-x)^{-\frac{1}{2}} e^{8(n+\frac{1}{2})^2 t^2/(x-t)} \tag{24}$$

or

$$\bar{C}(x, t; \infty) = \left(\frac{2}{\pi}\right)^{\frac{1}{2}} (t-x)^{-\frac{1}{2}} \Theta_2(0, e^{8t^2/(x-t)}), \tag{25}$$

where Θ_2 is the Jacobi theta-function. For $x < t$, the exponents are negative and the series (24) converges rapidly with the first term dominating as $x \to t$ from below. This solution was first found by Lighthill (1966) as an exact solution of the concentration equation far away from the tube walls. Results are plotted in figure 5(*a*, *b*) for $t =$ 0.05 and 0.1. Further results for larger values of t are plotted in figure 6(*a*, *b*); these are discussed in §7.

6.2. *Trailing-edge approximation*

The type II condition with Im $(a) \to \infty$ as $\lambda \to \infty$ implies that

$$\tau_1 e^{-2i\pi/3} = d_n,$$

where the d_n, $n = 0, 1, \ldots$, are the roots of $\mathrm{Ai}'(z) = 0$. After some manipulation, this case gives

$$\omega_n \to \mathrm{i}\lambda + d_n(4\mathrm{i}\lambda)^{\frac{2}{3}} \quad \text{as} \quad \lambda \to \infty \tag{26}$$

and branches 2, 3 and 5 on figure 1 are of this kind with $n = 0, 1, 2$ respectively. The associated eigenfunctions are found to be

$$\phi_n = \tau'(\sinh 2\theta)^{-\frac{1}{2}} \mathrm{Ai}(\tau'), \tag{27}$$

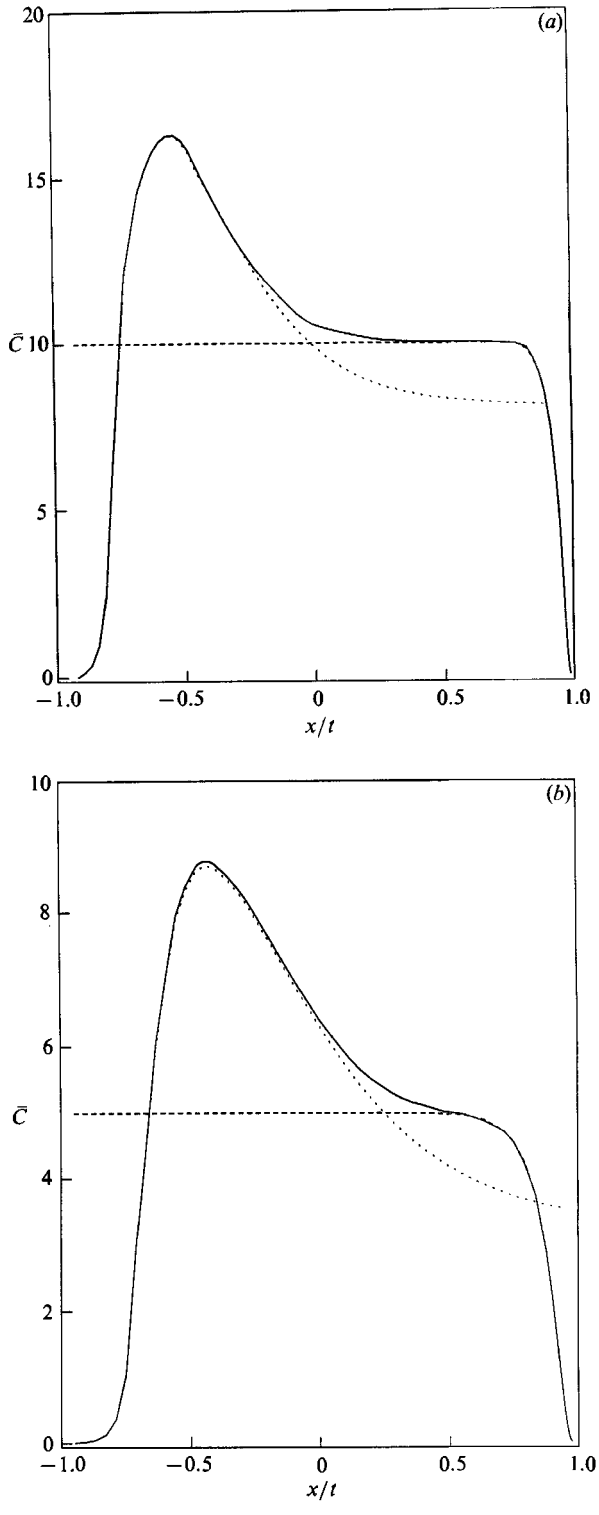

FIGURE 5. The two small-time approximations compared with the results of numerical integ at (*a*) $t = 0.05$ and (*b*) 0.1. ---, Lighthill approximation; ....., Airy approximation; —— profile.

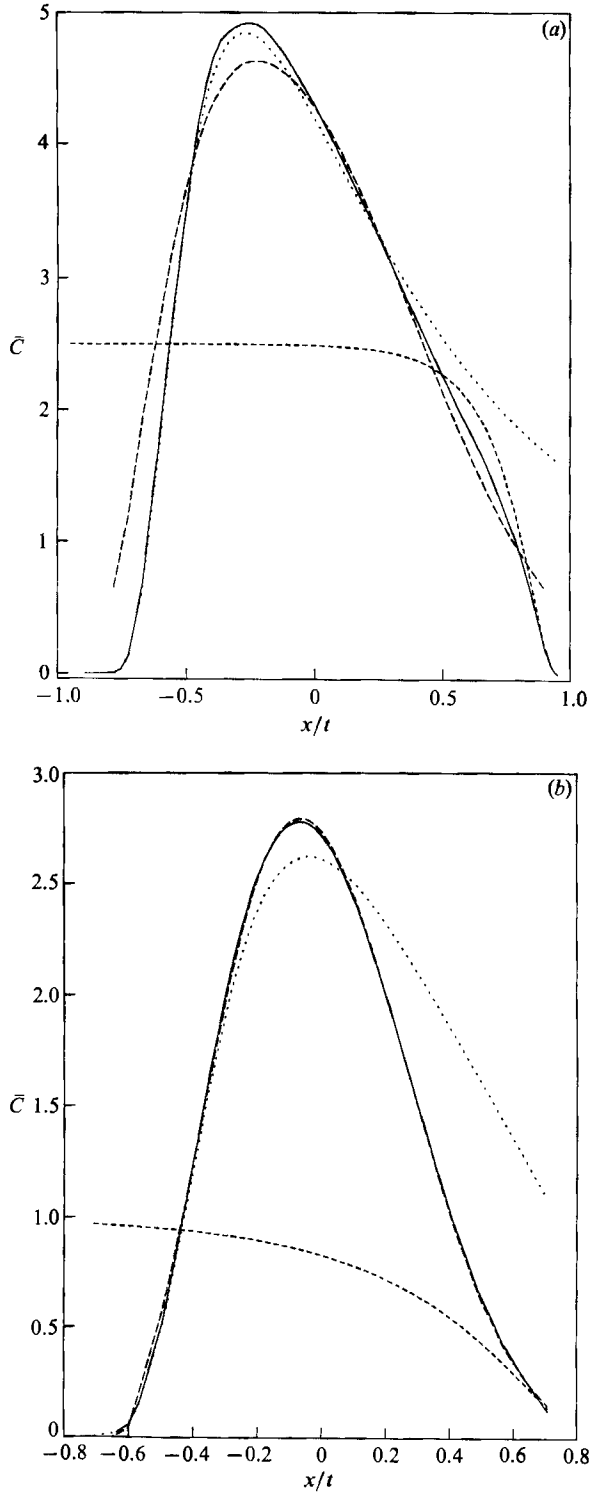

FIGURE 6. Large- and small-time approximations compared at (*a*) $t = 0.2$ and (*b*) $t = 0.5$ which are the margins of validity for each. ———, Taylor approximation; – – –, Lighthill approximation; ....., Airy approximation; ——, true profile.

with θ, τ' as defined in (20). These are oscillatory and largest near $r = 1$ which is the slowest moving part of the flow, and these eigenvalue branches describe the trailing edge of the solute cloud. For the case of $f(r, \lambda, 0) = 1$, substituting (26), (27) in (23) and finding the inverse Fourier transform of the residues F_n gives the result, to first order in t,

$$\bar{C}(x,t;\infty) = \sum_{n=0}^{\infty} \mathrm{e}^{-\frac{2}{3}h_n^3} \frac{3zv_n}{2t}(h_n \operatorname{Ai}(h_n^2) + \operatorname{Ai}'(h_n^2)), \tag{28}$$

where

$$z = t\left(\frac{4}{3(x+t)}\right)^{\frac{2}{3}}, \quad h_n = d_n z, \quad a_n = \operatorname{Ai}(d_n), \quad v_n = \frac{\int_{d_n}^{\infty} \operatorname{Ai}(s)\,\mathrm{d}s}{\mathrm{d}_n \operatorname{Ai}(d_n)}.$$

We believe that this expression (28) is new. It is generally very rapidly convergent over n, since the Airy function diminishes about as rapidly as the exponential factor.

The series can be improved by including extra terms in the expansion of the confluent hypergeometric function in terms of Airy functions. These expansions are analogous to the 'uniform asymptotic expansions' of the Bessel functions. Briefly, the expansions are of the kind

$$sF'(s) = c^{-\frac{1}{2}}(1 + 0.3c\tau + \ldots)\tau^{\frac{1}{4}} \operatorname{Ai}'(\tau) + (-0.3 - 0.030c\tau \ldots)\tau^{-\frac{1}{4}} \operatorname{Ai}(\tau),$$

$$F(s) = c^3(-0.078\,571 - \ldots)\tau^{\frac{1}{4}} \operatorname{Ai}'(\tau) + \tau^{-\frac{1}{4}} \operatorname{Ai}(\tau)(1 - 0.3c\tau + \ldots),$$

where $c = (1-2a)^{-\frac{2}{3}}$.

The approximations involve the integrals

$$I_j = \int_C m^j \mathrm{e}^{-m^{-3}/3 + h_i m^{-2}}\,\mathrm{d}m, \quad j \text{ a positive or negative integer.}$$

The contour C comes from infinity along the direction $\frac{1}{3}\pi$, and goes out to infinity along the direction $-\frac{1}{3}\pi$. The integrals satisfy the recurrence relation

$$I_{j+3} = 2h_i I_{j+2} + jI_j$$

and the differential relation

$$I_j' = I_{j+2}.$$

Initial values for I_{-1}, I_0 and I_1 are sufficient to generate all the terms. It is found that I_0 and I_1 can be expressed in Airy functions:

$$I_0(h) = \mathrm{e}^{-2h^3/2} \operatorname{Ai}(h^2), \quad I_1(h) = \mathrm{e}^{-2h^3/2}(h \operatorname{Ai}(h^2) + \operatorname{Ai}'(h^2)),$$

but I_{-1} is a little more difficult. We used a table of values obtained by solving the system of equations

$$I_{-1}' = I_1, \quad I_0' = I_2 = 2hI_1, \quad I_1' = I_3 = 2hI_0' + I_0.$$

As h increases from large negative values, the desired solution is the most rapidly increasing, and so can be obtained by solving from arbitrary starting conditions there, and multiplying by a normalizing factor to give the correct value at $h = 0$.

The first correction to the series (28) is therefore

$$\sum_{n=0}^{\infty} (z/t)^{\frac{1}{2}} v_n^2 d_n^{-1}[(0.9 + 1.8/v_n + 0.8d_n^3) I_0(h_n) + (1.8 - 0.8d_n^3) I_1(h_n)],$$

but the complexity of the succeeding corrections increases rapidly with increasing powers of $t^{\frac{1}{2}}$. We were able to obtain coefficients for the first nine corrections, i.e. up to and including $O(t^4)$, but fortunately, it is never necessary to sum over both many branches and many powers of $t^{\frac{1}{2}}$ at the same time. If t is other than very small, the

		Branch 1		
52.75265	0	0	0	0
19.85497	22.99164	0	0	0
−5.31640	3.72875	5.01032	0	0
7.39578	−1.45641	−0.26065	0.72790	0
−3.85532	4.67871	0.10006	−0.19378	0.07931
		Branch 2		
13.85667	0	0	0	0
−3.09629	10.15822	0	0	0
4.98973	−6.74996	3.72346	0	0
2.11450	12.72778	−4.11633	0.90988	0
−18.63423	−15.70065	8.71188	−1.40717	0.16676

TABLE 2. Table of coefficients c_{jk} for trailing-edge, small-time approximation.

minimum value of z in the range $-t < x < t$ is reasonably large, and only the first branch really matters. So we present, in table 2, some coefficients with the appropriate values of d_n, v_n, $n = 1, 2$ substituted. These values are:

$$d_1 = -1.018793, \quad v_1 = 1.48262, \quad d_2 = -3.24820, \quad v_2 = -0.759842.$$

The coefficients, denoted c_{jk} in the usual matrix convention, are to be used in the formula

$$\bar{C}(x, t; \infty) = \frac{h_1^2}{16t} \sum_{j=0}^{\infty} \sum_{k=0}^{j} c_{jk} \left(\frac{4t}{h_1 d_1^2} \right)^{j/2} I_{2k+1-j}(h_1). \tag{29}$$

The results are shown in figures 5 and 6, and discussed in the next section.

7. Discussion of approximations and conclusion

We have extended the large-time Taylor–Chatwin approximation for dispersion in Poiseuille flow and introduced a new approximation, valid near the trailing edge, to complement the known small-time approximation near the leading edge. These approximations are compared in figures 4–6 with the numerical solutions obtained using the spectral method. Between them, the approximations predict all the qualitative features of the flow, and at least one of them is effective at all parts of the profiles at all times. The crossover region is in the neighbourhood of $t = 0.2$. For $t < 0.1$, the small-time approximations (24), (28), (29) are satisfactory, and for $t > 0.5$, the extended large-time approximation (19) is entirely adequate.

The large-time approximation eventually fails primarily because it is based on a power series expansion on a surface which inevitably has branch points. It is a divergent asymptotic series. It is also an expansion based on only one of the saddle points; there are others on other branches. The limiting effect of the branch points is more important at small times, however, and it is not necessary to examine saddle points other than the first.

The small-time approximations are limited essentially because they are based on eigenvalue solutions based on one or other boundary of the ordinary differential equation (o.d.e.) (3), assuming the other is at infinity. They fail when material reflected from this boundary becomes important. So, although the convergence of the series (24) and (28) over time is quite satisfactory, there is an error which cannot be removed by just taking more terms.

Of the two small-time approximations, the new trailing-edge one seems much the

more useful. That is partly because the more obvious features of the profile occur in this trailing region. Moreover, it is clear from figure 6 that the crossover region in effectiveness lies well forward of the midpoint of the profile, and that only the trailing-edge expression comes close to approximating the eventual Gaussian shape.

We have shown that Fourier transformation, coupled with use of residue calculus in the complex plane of the transformation parameters, gives a quick and accurate numerical method of calculating the averaged profiles. With further analysis, the method yields reasonably accurate approximations which cover the entire domain on which solutions may be needed. The results are specialized to the case of uniform initial delta-function distribution and infinite Péclet number. It is time to review these assumptions to see how restrictive they are.

The assumption of infinite Péclet number, equivalent to ignoring longitudinal diffusion, creates no problem. As explained in §3, restoration of finite Péclet number requires only a convolution with an appropriate Gaussian, i.e. a smoothing operation. More general initial distributions, uniform across the cross-section, can be treated by using the solution described here as a Green function. The restriction to cross-sectionally averaged solutions was necessary for the presentation of results to avoid dealing with the radial distance as an extra variable, but there is no difficulty in principle with calculating the pointwise solutions, either by the approximations of §§5 and 6, or the numerical method of §3.

An initial distribution that is not uniform across a section, but is still radially symmetric, is also explicitly provided for by the method of this paper. A distribution without radial symmetry, though, would introduce a third space variable, creating a need to invert a triple integral transform. We would approach this task with trepidation.

One might wonder whether flows of other cross-sections could be treated in the same way. An important feature of our original partial differential equation (1) is that the coefficients depend on only one of three independent variables, leaving an o.d.e. to analyse after integral transformation. The fact that this o.d.e. is the well-known confluent hypergeometric equation is not critical; the methods of saddle-point approximation and turning-point analysis used are quite general. But if the coefficients depend on more than one variable in such a way that the equation after integral transformation remains a partial differential equation, in a reduced number of variables, then the prospect for approximation is less promising. Nevertheless, if the dimension of the transformed problem is even one less, the numerical procedure of solving this problem, and inverting the integral transformation by residue calculus may be appealing.

As well as presenting a useful numerical method, we have sought in this paper to show that there is a real link between the structure of the implicit function of the two transform variables and the physical characteristics of the flow. This is reflected in the different regions of utility of the approximations based on different regions of the transformed domain. There is every reason to expect a corresponding association in any other flow for which a similar transformation is possible. That means that short-time behaviour, which is necessarily local, will be of different type in different flow regions, and each different type will correspond to a different kind of asymptotic behaviour in the far field of the transformed variables. Correspondingly the long-term behaviour, when different flow regions have had the opportunity to affect each other, will be explained by the near-zero behaviour in the transformed plane. It is worth remarking that although attention has been paid to the branch points in the expression of one variable as a function of another, their role is that of a mechanical

inconvenience and a reflection of the presence of transition from one type of asymptotic behaviour to another, rather than as reflecting physically important characteristics in themselves.

REFERENCES

ABRAMOWITZ, M. & STEGUN, I. A. 1965 *Handbook of Mathematical Functions*. Dover.

ARIS, R. 1956 On the dispersion of a solute in a fluid flowing through a tube. *Proc. R. Soc. Lond.* A **235**, 67–77.

BARTON, N. G. 1983 The dispersion of solute from time-dependent releases in parallel flow. *J. Fluid Mech.* **136**, 243–267.

BARTON, N. G. & STOKES, A. N. 1986 A computational method for shear dispersion in parallel flow. In *Proc. Computational Techniques and Applications Conf., CTAC-85* (ed. J. Noye & R. May), pp. 345–355. North-Holland.

CHATWIN, P. C. 1970 The approach to normality of the concentration distribution of a solute flowing along a straight pipe. *J. Fluid Mech.* **43**, 321–352.

CHATWIN, P. C. 1973 On the longitudinal dispersion of dye whose concentration varies harmonically with time. *J. Fluid Mech.* **58**, 657–667.

GANCE, A. E. DE & JOHNS, L. E. 1978*a* The theory of dispersion of chemically active solutes in a rectilinear flow field. *Appl. Sci. Res.* **34**, 189–225.

GANCE, A. E. DE & JOHNS, L. E. 1978*b* On the dispersion coefficients for Poiseuille flow in a circular cylinder. *Appl. Sci. Res.* **34**, 227–258.

GILL, W. N. & ANANTHAKRISHNAN, V. 1967 Laminar dispersion in capillaries. Part 4. The slug stimulus. *AIChE J.* **13**, 801–807.

GILL, W. N. & SANKARASUBRAMANIAN, R. 1970 Exact analysis of unsteady convective diffusion. *Proc. R. Soc. Lond.* A **316**, 341–350.

HOUSEWORTH, J. E. 1984 Shear dispersion and residence time for laminar flow in capillary tubes. *J. Fluid Mech.* **142**, 289–308.

JAYARAJ, K. & SUBRAMANIAN, R. S. 1978 On relaxation phenomena in field-flow fractionation. *Sep. Sci. Tech.* **13**, 791–817.

LIGHTHILL, M. J. 1966 Initial development of diffusion in Poiseuille flow. *J. Inst. Maths Applics.* **2**, 97–108.

PHILIP, J. R. 1963*a* The theory of dispersal during laminar flow in tubes. I. *Austral. J. Phys.* **16**, 298–299.

PHILIP, J. R. 1963*b* The theory of dispersal during laminar flow in tubes. II. *Austral. J. Phys.* **16**, 300–310.

SMITH, R. 1981 A delay-diffusion description for contaminant dispersion. *J. Fluid Mech.* **105**, 469–486.

SMITH, R. 1987 Diffusion in shear flows made easy: the Taylor limit. *J. Fluid Mech.* **175**, 201–214.

STOKES, A. N. & BARTON, N. G. 1985 Solution of dispersion in Poiseuille flow by integral transforms. *Third Australasian Conf. on Heat and Mass Transfer, University of Melbourne*, pp. 217–224.

TAYLOR, G. I. 1953 Dispersion of soluble matter in solvent flowing slowly through a tube. *Proc. R. Soc. Lond.* A **219**, 186–203.